Contents lists available at ScienceDirect

Computers & Graphics

journal homepage: www.elsevier.com/locate/cag

Multi-resolution Terrain Rendering Using Summed-Area Tables Supplemental Material

Shi Li, Chuankun Zheng, Rui Wang*, Yuchi Huo, Wenting Zheng, Hai Lin, Hujun Bao

State Key Lab of CAD&CG, Zhejiang University, HangZhou, 310058, China

ARTICLE INFO

Article history:
Received 2021

Keywords: Terrain Rendering, Summed-Area Tables (SATs), Level of Detail (LOD)

ABSTRACT

Due to the fundamental weaknesses of level-of-detail (LOD) control and rich details in the Geometry Clipmaps, we propose a multi-resolution terrain rendering algorithm that utilizes summed-area tables (SATs) [1] to facilitate the rendering of terrain with better geometric and shading details. First, our algorithm introduces a novel geometric error bound on the screen-based terrain rendering approach that juggles low rendering throughput and better LOD control. Geometric errors are estimated in real-time from SATs, enabling error-bounded geometry clipmap. Second, we utilize Spherical Gaussian (SG) functions to approximate lighting and bidirectional reflection distribution functions (BRDFs), and efficiently calculate outgoing radiance with self-occlusions of the terrain. SATs are utilized to enable the mipmapping of visibility and normal maps. We demonstrate the improvements of our method with experiments on accuracy and efficiency.

Appendix A. Terrain Integration

The outgoing radiance on point x toward direction ω_o is calculated as [2]:

$$L_o(x,\omega_o) = \int_{S^2} L_i(x,\omega_i)\rho(x,\omega_i,\omega_o)\langle n(x),\omega_i\rangle d\omega_i, \quad \text{(A.1)}$$

where ω_i is the incident direction, S^2 represents the hemisphere, $L_i(\omega_i)$ denotes the incident radiance, ρ shows the BRDF, $n(x)$ stands for normal vector at point x, the operator $\langle\cdot,\cdot\rangle$ gives the dot product of two vectors, clamped to zero if it is negative. Considering the filtering of nearby samples on the heightmap get the an antialiased integration over the footprint Ω around the point x [3]:

$$L_o(\Omega,\omega_o) = \frac{1}{|\Omega|}\int_\Omega\int_{S^2} L_i(y,\omega_i)\rho(y,\omega_i,\omega_o)V(y,\omega_i) \langle n(y),\omega_i\rangle d\omega_i dy, \quad \text{(A.2)}$$

where $|\Omega|$ denotes the surface area of Ω and $V(y,\omega_i)$ is the visibility term representing whether local geometry cast shadows at point y from direction ω_i.

Han et al. [4] assumed that $L(y,\omega) \approx L_i(x,\omega)$ for all $y \in \Omega$ and $\omega \in S^2$ when Ω is small neighbor around x to simplify Equation as:

$$L_o(\Omega,\omega_o) = \int_{S^2} L_i(x,\omega_i)\bar{\rho}(\omega_i,\omega_o)d\omega_i, \quad \text{(A.3)}$$

where $\bar{\rho}$ is the effective BRDF [4] given by

$$\bar{\rho}(\omega_i,\omega_o) = \frac{1}{|\Omega|}\int_\Omega \rho(y,\omega_i,\omega_o)V(y,\omega_i)\langle n(y),\omega_i\rangle dy \quad \text{(A.4)}$$

Previous works[5, 3] have proved that separating the shadow term with the normal and BRDF can achieve an accurate approximation of Equation A.5 as:

$$\begin{aligned}\bar{\rho}(\omega_i,\omega_o) &= \bar{\rho}_n(\omega_i,\omega_o)\bar{\rho}_v(\omega_i),\\ \bar{\rho}_n(\omega_i,\omega_o) &= \frac{1}{|\Omega|}\int_\Omega \rho(y,\omega_i,\omega_o)\langle n(y),\omega_i\rangle dy,\\ \bar{\rho}_v(\omega_i) &= \frac{1}{|\Omega|}\int_\Omega V(y,\omega_i)dy.\end{aligned} \quad \text{(A.5)}$$

*Corresponding author: Tel.: +86-0571-88206681-430;
e-mail: rwang@cad.zju.edu.cn (Rui Wang)

Thus, we can derive our shading equation with Equation A.3 and A.5:

$$L_o(\Omega, \omega_o) = \int_{S^2} L_i(x, \omega_i)\bar{\rho}_n(\omega_i, \omega_o)\bar{\rho}_v(\omega_i)d\omega_i. \tag{A.6}$$

Appendix B. vMF based Approximation

In order to efficiently calculate the integration, we use different approaches to approximate $\bar{\rho}_n$ and $\bar{\rho}_v$. For $\bar{\rho}_n$, a specular BRDF term can be represented using the vMF distribution [4, 6] as follows:

$$\begin{aligned} \bar{\rho}_n(\omega_i, \omega_o) &= \frac{1}{N}\sum_{j=0}^{N} vMF(\omega_h; \mu_j, \kappa_j) \\ vMF(\omega; \mu, \kappa) &= \frac{\kappa}{4\pi sinh(\kappa)} e^{\kappa(\mu \cdot \omega)}, \end{aligned} \tag{B.1}$$

where $\omega_h = (\omega_i + \omega_o)/||\omega_i + \omega_o||$ is the half-vector, N is the number of discrete texels in footprint Ω, $\mu_j \in S^2$ is the direction of a lobe, and $\kappa_j \in R_+$ is the glossiness of a lobe. When $\kappa_j >> 1$, Equation B.1 can be approximated with a normalized SG function:

$$vMF(\omega; \mu, \kappa) = \frac{\kappa}{2\pi} e^{\kappa(\mu \cdot \omega - 1)}. \tag{B.2}$$

Similarly, Wang et al. [7] adopted SG functions to represent a diffuse BRDF by substituting $\rho(y, \omega_o, \omega_i) = \frac{1}{\pi}$ in Equation A.5:

$$\bar{\rho}_n(\omega_i, \omega_o) = \frac{1}{N}\sum_{j=0}^{N} 1.170 e^{2.133(\omega_i \cdot n(y_j) - 1)}, \tag{B.3}$$

Therefore, we could give a unified expression to represent the average BRDF based on vMF distributions as follows:

$$\bar{\rho}_n(\omega_i, \omega_o) = \frac{1}{N}\sum_{j=0}^{N} vMF(\omega_i, \omega_o; \mu_j, \kappa_j). \tag{B.4}$$

Appendix C. vMF Lobes Merging

Because the large number of vMF lobes in ρ_n at each footprint can cause heavy integration overhead at runtime, we adapt vMF merging technique to reduce the size [6]. Xu et. al [6] introduced an unnormalized vector $r \in R^3$ to characterize a vMF distribution. These vectors can be merged into one or multi merged vMF lobes to accelerate the integration over the pixel footprint. Specifically, the mapping between a vMF and a vector r can be calculated as follows:

$$\frac{r}{||r||} = \mu, \frac{3\,||r|| - ||r||^3}{1 - ||r||^2} = \kappa. \tag{C.1}$$

Therefore, we could replace the presentation $vMF(\omega; \mu, \kappa)$ in Equation B.4 with $vMF(\omega; r)$.

$$\bar{\rho}_n(\omega_i, \omega_o) = \frac{1}{N}\sum_{j=0}^{N} vMF(\omega_h; r_j), \tag{C.2}$$

The merging of multiple lobes, i.e., vector r_j, can be calculated by a simple average of vectors:

$$r_M = \frac{1}{N}\sum_{j=0}^{N} r_j, \tag{C.3}$$

where r_M is the merged lobe. The original parameters(μ and κ) of a vMF distribution can be obtained from r_M(see Xu et al. [6] for more details).

Thus, we use a similar method to acquire the average BRDF over the pixel footprint Ω from Equation C.2.

$$\bar{\rho}_n(\omega_i, \omega_o) = vMF(\omega_i, \omega_o, r_M) \tag{C.4}$$

with r_M is the average vMF distribution.

Appendix D. Additional Result

In order to demonstrate the shading effects of our error-bound method, we construct a heightmap with more cliffs and details using a terrain generator with Perlin Noise. As shown in Figure D.1, our method depicts mountain gullies and ridges vividly, while Geometry Clipmaps [8, 9] overly smoothens the mountains' contour lines.

References

[1] Crow, FC. Summed-area tables for texture mapping. In: ACM SIGGRAPH computer graphics; vol. 18. ACM; 1984, p. 207–212.
[2] Kajiya, JT. The rendering equation. In: ACM Siggraph Computer Graphics; vol. 20. ACM; 1986, p. 143–150.
[3] Dupuy, J, Heitz, E, Iehl, JC, Poulin, P, Neyret, F, Ostromoukhov, V. Linear efficient antialiased displacement and reflectance mapping. ACM Transactions on Graphics (TOG) 2013;32(6):211.
[4] Han, C, Sun, B, Ramamoorthi, R, Grinspun, E. Frequency domain normal map filtering. ACM Transactions on Graphics (TOG) 2007;26(3):28.
[5] Bruneton, E, Neyret, F. A survey of nonlinear prefiltering methods for efficient and accurate surface shading. IEEE Transactions on Visualization and Computer Graphics 2012;18(2):242–260.
[6] Xu, C, Wang, R, Zhao, S, Bao, H. Real-time linear brdf mip-mapping. In: Computer Graphics Forum; vol. 36. Wiley Online Library; 2017, p. 27–34.
[7] Wang, J, Ren, P, Gong, M, Snyder, J, Guo, B. All-frequency rendering of dynamic, spatially-varying reflectance. In: ACM Transactions on Graphics (TOG); vol. 28. ACM; 2009, p. 133.
[8] Asirvatham, A, Hoppe, H. Terrain rendering using gpu-based geometry clipmaps. GPU gems 2005;2(2):27–46.
[9] SONG, G, YANG, H, JI, Y. Geometry clipmaps terrain rendering using hardware tessellation. IEICE Transactions on Information and Systems 2017;E100.D(2):401–404.

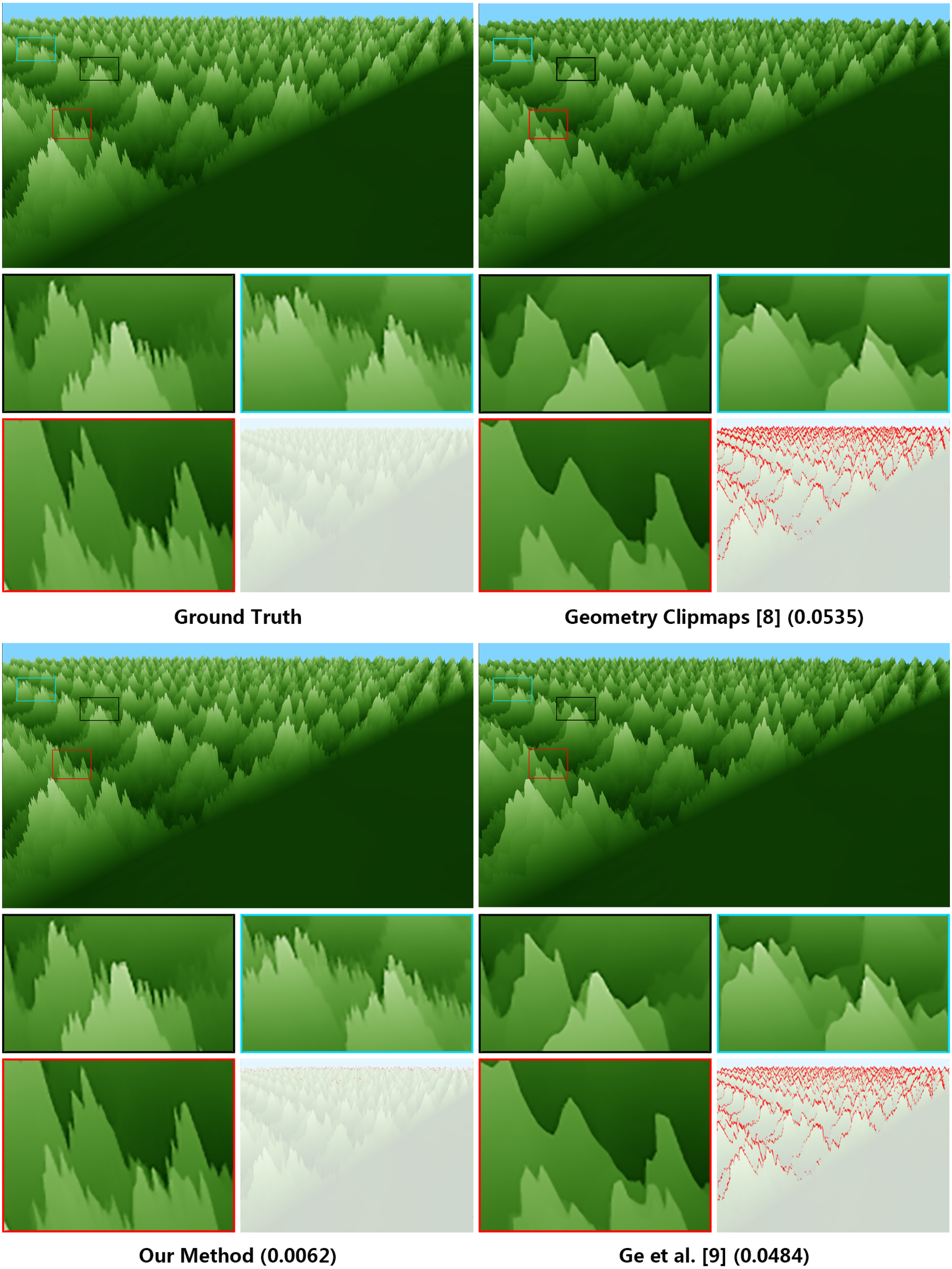

Fig. D.1. Comparison of geometric details between Our Methods, Geometry Clipmaps [8] and Ge et al. [9]. The RMSE values are shown in the bracket.